Available online at www.sciencedirect.com
SCIENCE DIRECT®
International Journal of Multiphase Flow 30 (2004) 939–961
International Journal of Multiphase Flow
www.elsevier.com/locate/ijmulflow

The wake effect on bubble rising velocity in one-component systems ☆

Gian Piero Celata [a,*], Maurizio Cumo [b], Francesco D'Annibale [a], Akio Tomiyama [c]

[a] *ENEA, Institute of Thermal-Fluid Dynamics, Rome Italy, Via Anguillarese, 301, Rome, Italy*
[b] *University of Rome 'La Sapienza', DINCE, Rome, Italy, Corso V. Emanuele 244, Rome, Italy*
[c] *Kobe University, Graduate School of Science and Technology, Rokkodai, Nada, Kobe, Japan*

Received 4 September 2003; received in revised form 28 April 2004

Abstract

The present paper reports an experiment of bubble rising velocity in a liquid column using R-114 and FC-72. Vapour bubbles are generated at the bottom of the saturated liquid column by a tiny electric heater and their evolution is recorded with high speed cinematography from the generation point until they reach the terminal velocity in the liquid column.

Single bubble and bubble train (with controlled frequency) tests are carried out to ascertain the wake effect on the bubble rising velocity in the range of bubble diameter from 0.1 to 0.7 mm, showing a negligible wake effect on the tested bubbles.

Prediction of bubble terminal rising velocity with available correlations has been attempted. Though most of them have been developed for two-component systems (gas and liquid), some of them provide with a fairly good prediction. A recent drag coefficient model, specifically derived for distorted spheroidal bubbles in infinite stagnant liquids under a surface tension dominant regime, looks promising although the agreement with the present experimental data is not completely satisfactory, as being similar to Fan and Tsuchiya correlation.

A reasonable prediction of bubble shape has been obtained using available correlations and models, and specifically the Taylor and Acrivos model and the Vakhrushev and Efremov correlation.

☆ Authors are happy to express their wishes to George Yadigaroglu, one of the most outstanding personality in the heat transfer and multiphase flow field, and to contribute to this Festschrift in his honour. Friendship with George started many years ago and this has been a great chance for all of us. We do hope this occasion to be a starting point rather than an arrival point, and we wish George continued professional success, good health, and happiness in the years to come.

* Corresponding author.

0301-9322/$ - see front matter © 2004 Published by Elsevier Ltd.
doi:10.1016/j.ijmultiphaseflow.2004.04.007

Keywords: Wake effect; Bubble terminal velocity; Refrigerants; Bubble frequency; One-component system

1. Introduction

As is known, bubble rising velocity in a stagnant liquid column is governed by buoyancy and drag forces. These forces strongly depend on fluid properties and gravity (both) as well as on the bubble equivalent diameter and degree of contamination on the gas–liquid interface (drag force).

Detailed information on the motion of gas bubbles in a liquid, both experimental and theoretical, is available in the literature (Peebles and Garber, 1953; Kupferberg and Jameson, 1969; Satynarayan et al., 1969; Tsuge and Hibino, 1972; Grace et al., 1976; Wallis, 1969; Bhaga and Weber, 1981; Tsuge, 1986; Tomiyama, 1998; Tomiyama et al., 1998a,b, Fan et al., 1999, Ruzicka, 2000, Di Marco et al., 2003, Okawa et al., 2003, among the others, being not possible to be exhaustive here). All of these studies have been performed using two-component immiscible fluids (gas into liquid), in adiabatic conditions. Besides, most of them are related to the motion of air bubbles in water or water-based mixtures. Only a few works have been focused on different fluids, such as the works carried out by Tadaki and Maeda (1961), Park et al. (1977) and Tsuge and Hibino (1972), and, as far as known, none of them on organic refrigerants. Good reviews on the subject were compiled by Clift et al. (1978), Tsuge (1986), and Fan and Tsuchiya (1990). Nonetheless, there is an obvious lack of information on bubble rising velocity in one-component systems, where bubbles are generated by the boiling of the liquid (diabatic conditions), as only very few works are available: Vassallo et al. (1995) measured the bubble rise velocity of R114 vapour bubbles in the same liquid at about 24.5 °C and 0.21 MPa; Okawa et al. (2003) carried out some tests of steam bubbles rising in water at about 100 °C and atmospheric pressure.

The study of terminal bubble rising velocity in a one-component system is of importance for different reasons. It is possible to change the saturated vapour density (acting on the pressure) much more than what is possible in a gas–liquid system, and therefore one can get a wider range of $\Delta\rho$ (data are also of interest for microgravity conditions). Such a possibility will be used in a further work, in the frame of a wider research in this topic, where it is studied the bubble behaviour up to the critical pressure, while in the present paper the attention is only paid at the wake effect for small bubbles at low pressure.

The behaviour of the interface is not identical, as for one-component systems also at the equilibrium there is always a molecular mass transfer between liquid and vapour. The situation is closer to the actual one where bubble are obtained by boiling; therefore, at the latest, one could get the confirmation or not of the analogy between gas and vapour bubbles.

Recently, Celata et al. (2001a,b) measured bubble terminal rising velocities in one-component systems using FC-72 and R-114, in order to obtain a consistent data set up to the critical pressure. The knowledge of bubble dynamics as a function of the system pressure, up to the critical pressure, is of interest in many applications, such as bubbles under microgravity conditions. In the experiments described in Celata et al. (2001a,b), bubbles were generated as a bubble train, the frequency of which could not be controlled. In this case, because of the short distance between two adjacent bubbles, the terminal rising velocity of a bubble may be affected (increased) by the

wake of the bubbles preceding it, as clearly evidenced by Tsuge and Hibino (1972), and treated by Fan and Tsuchiya (1990), as examples. On the other hand, Marks (1973) experienced the absence of the wake effect for air bubbles in water, when the bubble diameter was less than 1.2 mm. The range of vapour bubble diameter in Celata et al. (2001a,b) experiment was less than 1.0 mm.

Katz and Menevau (1996) experienced a wake effect for very small air bubbles in distilled water at small Eötvös number, Eo ($=(\rho_l - \rho_g)gd^2/\sigma$, where ρ_l and ρ_g are the liquid and vapour density, respectively, g the gravity acceleration, d the equivalent bubble diameter and σ the surface tension) ($Eo < 0.3$) and small Reynolds number, Re ($=\rho_l V_T d/\mu_l$, where V_T is the terminal velocity, and μ_l is the liquid viscosity) ($Re < 35$). However, these data are characterized by air bubble pairs, i.e., a condition which is quite different from Tsuge and Hibino (1972) and Marks (1973) data. Therefore, a comparison between these two series of data cannot be made in a homogeneous way.

In order to have an experimental evidence of the wake effect on bubbles trains in this range of bubble diameter and to extend the observations by Tsuge and Hibino (1972) to smaller bubble diameters, a simple experiment has been carried out in this study, where single bubbles or bubble trains with variable (imposed) frequency are generated, and the experimental results will be described in the following. As it will be described later in detail, bubbles generated in the present experiment are in thermodynamic equilibrium with the surrounding liquid.

2. Experimental apparatus

The experimental facility shown schematically in Fig. 1 consists of a rectangular test section, a fluid-storage tank, a high-speed video camera (Speedcam 512 Weinberger, 1000 fps, at a resolution of 512×512 pixel), a stroboflash light (Kodak, duration of the flash about 20 μs), a data acquisition system (Labview software) and an image digital treatment system (Labview/Imaq software). The rectangular test section is made up of an insulated brass vessel with heated walls (to heat the wall and fluid at a test temperature, and to compensate heat losses during the test; its inner volume filled with the test fluid is about 1 dm^3, the maximum pressure is 5.0 MPa while the maximum temperature is 180 °C); glass windows on the four sides of the test section which allow complete visualization of bubbles with the high-speed video camera and the stroboflash light,

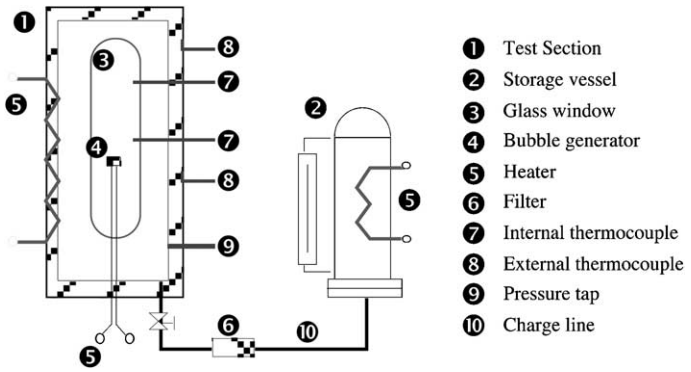

Fig. 1. Schematic of the experimental apparatus and the test section.

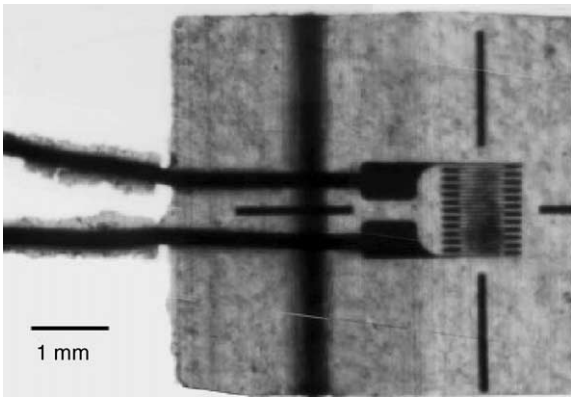

Fig. 2. Picture of the heating element used for the generation of single bubbles and controlled frequency bubbles.

instrumentation such as thermocouples and pressure transducers and a system for generating saturated vapour bubbles. This system, a picture of which is shown in Fig. 2, is made up with a small thin-film electric resistance (actually a component of a strain-gauge typically used for manufacturing pressure transducers), which is flush-mounted in horizontal position inside the saturated liquid with the heating element upwards, a waveform generator (Hewlett-Packard HP33120A), and a power amplifier (MB-Electronics, 2250 MB). The electric resistance of the heating element is 120 Ω and its size is 1.2×1.0 mm. Supplying the resistance with a voltage can produce bubbles at the top of the heater. With a single voltage pulse we can generate a single bubble, while if we supply the electric resistance with pulse (voltage) trains we can produce bubbles with different frequencies, depending on the applied pulse frequency. The lasting of the electric pulse is 1 ms, the width ranges from 10 to 30 V, and the frequency, which affects the distance between two adjacent bubbles, from 1 to 150 Hz. Refrigerants FC-72 and R-114 are used as fluids.

As the liquid in the test section is under saturated conditions before the test, the additional heating coming from the electrical resistance causes the evaporation of the liquid on the surface of the heater. Wall insulation makes the test section an adiabatic system (towards the external ambient). Therefore, we do not have a significant convective motion or liquid stratification, as also confirmed by the measurement provided by the two thermocouples placed in two different positions inside the liquid column (top and bottom of the test section).

The process fluid, either FC-72 or R-114, is degassed. The method employed for the filling of the test section and the preparation of the test ensures instead a high degree of liquid degassing. The liquid is boiled up in the storage tank (2 in Fig. 1) to pressurize it and allow its transfer (drainage is from the bottom) to the test section (1 in Fig. 1). The test section is filled up completely and liquid brought to boiling for further degassing. Then, the valve on the dome is closed and the test section is pressurized with its own vapour pushing some liquid in the storage tank. After the tests the process liquid is drained completely in the storage tank taking advantage of the vapour pressure in the test section and eventually insulated. Therefore the process liquid in the storage tank is always degassed and possible small air contaminations (which could occur only on the liquid surface in the test section during the refill stage) are immediately eliminated from liquid boiling and from the vapour purge before leading the facility in steady state conditions.

Bubble motion in the liquid column is recorded with the high-speed video camera for few seconds (4–8 s) from the heater up to the liquid free surface. A selected sequence of frames (about 100 consecutive frames) are then analyzed with the image digital treatment system. The program is able to recognize each bubble, providing with the trajectory, the velocity, the shape, the dimensions, and the volume. The volume is derived from the cross-sectional area and the axes of a bubble, assuming a spheroidal shape. Bubble volume is not obtained from a single image but considering the average along the whole path, then considering some tens of images.

3. Experimental results

3.1. Experimental uncertainty

The uncertainty in the evaluation of the bubble terminal velocity is due to two contributions. The first contribution, very small, is due to the error in the digital image procedure. The maximum uncertainty is 2 pixels, and considering that we use 2/3 of the screen, i.e., 340 pixel out of 512, the maximum error is ±0.6%. This uncertainty is the only one for the velocity mean value, i.e., the single data point in Fig. 7. The second contribution is due to the velocity oscillation around the mean terminal velocity, as shown in Fig. 6, and is mainly due to the limited number of points used for the average calculation. It has been evaluated as ±4.6%, for a total error of ±5.2%.

As far as the bubble diameter is concerned, the major source of uncertainty is the definition of the threshold in the setting of the digital image system. Assuming a maximum error of ±1 pixel in the definition of the contour of the bubble, we have that the average error in the diameter calculation is ±3.6% (from ±1.8% to ±8.0%) for FC-72 (75 data points) and ±7.0% (from ±3.0% to ±12.0%) for R-114 (77 data points). The error is an increasing function of the pressure, mainly because of the reduction in the bubble diameter as the pressure increases.

The uncertainty in the bubble shape has been calculated considering for each bubble the root mean square of the aspect ratio along the observed path of the bubble. This will, of course, keep into account possible bubble oscillations and changes due to the helical or zigzag motion, as well as the error in digital processing (±1 pixel) and will lead to an overestimation of the error. In summary, the average rms is ±2.9% (from ±1.2% to ±5.3%) for FC-72 and ±3.2% (from ±0.8% to ±5.9%) for R-114.

3.2. Discussion

As already mentioned, Tsuge and Hibino (1972) showed the influence of the wake effect on bubble rising velocity for air bubbles having a diameter ranging from 5 to 9 mm, in water. Tsuge and Hibino results are reproduced in Fig. 3, in which the bubble rising velocity, V_T (normalized against the single bubble velocity, V_o) is plotted against the distance between two adjacent bubbles, z (normalized against the equivalent bubble diameter, d). This is the distance between the bubble centres. The wake effect is definitely relevant for such large bubbles, being remarkable even for large distances between two adjacent bubbles (greater than 10% for z/d around 35). It is clear from the figure that the wake effect sharply reduces as d decreases from 9 to 5 mm. Judging from the results of Marks (1973), whose measurements of air bubbles in distilled water showed that the

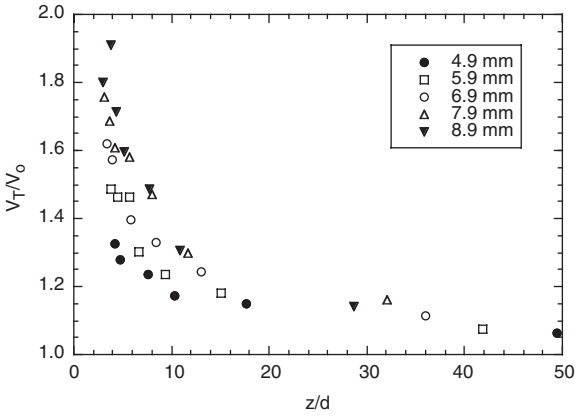

Fig. 3. Wake effect after Tsuge and Hibino (1972): bubble terminal rising velocity versus the distance between two adjacent bubbles (in bubble diameters).

increase of velocity with frequency was inversely related to bubble size until it was negligible for smaller bubbles (diameter smaller than 1.2 mm), we might expect that for bubbles with a diameter smaller than 1.0 mm, the wake effect may be negligible.

Vapour bubbles obtained in the present work, using both FC-72 and R-114, have a diameter ranging from 0.2 to 0.7 mm, and a reduced pressure of 0.06–0.15 for FC-72 and 0.08–0.29 for R-114. Frequency controlled tests provide bubbles characterized by a frequency ranging between 1 and 150 bubble/s, while the corresponding distance between adjacent bubbles ranges between 3

Table 1
Main physical properties of FC-72 and R-114

T (°C)	p (bar)	Reduced pressure	ρ_L (kg/m^3)	ρ_V (kg/m^3)	h_{LV} (kJ/kg)	μ_L (kg/ms)	μ_V (kg/m s)	σ (N/m)
R-114								
30	2.500	0.0744	1440.8	18.38	126.3	3.24e−04	1.20e−05	1.03e−02
40	3.372	0.1004	1408.9	24.50	122.1	2.91e−04	1.23e−05	9.20e−03
50	4.454	0.1326	1375.4	32.13	117.5	2.64e−04	1.26e−05	8.14e−03
60	5.775	0.1719	1340.1	41.55	112.7	2.40e−04	1.30e−05	7.12e−03
70	7.364	0.2192	1302.7	53.15	107.4	2.20e−04	1.35e−05	6.12e−03
80	9.254	0.2754	1262.6	67.41	101.7	2.00e−04	1.40e−05	5.14e−03
84	10.000	0.2976	1247.7	73.20	99.6	1.96e−04	1.42e−05	4.81e−03
FC-72								
55	0.960	0.0522	1622.6	12.74	85.0	4.61e−04	9.60e−06	8.41e−03
60	1.124	0.0611	1613.7	14.79	83.6	4.39e−04	9.71e−06	7.98e−03
65	1.336	0.0726	1603.5	17.52	82.1	4.18e−04	9.81e−06	7.56e−03
70	1.549	0.0842	1593.3	20.24	80.6	3.98e−04	9.92e−06	7.15e−03
75	1.818	0.0988	1581.1	23.72	79.1	3.80e−04	1.00e−05	6.74e−03
80	2.088	0.1135	1569.0	27.20	77.5	3.62e−04	1.01e−05	6.33e−03
85	2.425	0.1318	1554.1	31.59	75.9	3.43e−04	1.02e−05	5.93e−03
90	2.761	0.1501	1539.2	35.98	74.4	3.25e−04	1.04e−05	5.54e−03

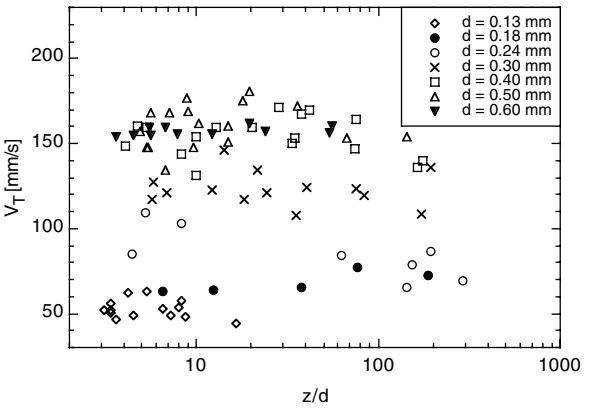

Fig. 4. Bubble terminal rising velocity as a function of the distance between two adjacent bubbles, given in bubble diameters, for different bubble diameter.

and 300d. The Reynolds number ranges from 60 to 435 for FC-72 data and from 35 to 400 for R-114 data. Main physical properties of FC-72 and R-114 are reported in Table 1. Experimental data are shown in Fig. 4 where the bubble rising velocity, V_T, is plotted against z/d. The equivalent bubble diameter reported on the figure is the nominal one which is used to give an idea of the order of magnitude of bubbles. The nominal diameter implies bubbles having a diameter ranging from ± half of the contiguous ranges, i.e., $d = 0.30$ mm groups bubbles from $d = 0.27$ mm to $d = 0.35$ mm. Extremal groups comprise also all bubbles smaller than 0.13 mm and larger than 0.60 mm.

We are therefore dealing with a bubble diameter which is more than an order of magnitude less than Tsuge and Hibino data, and also smaller than Marks bubbles diameter. Looking at present data no increase in the rising velocity is observed as the distance between bubbles decreases. From this observation we may conclude that the wake effect for this range of bubble diameter cannot be detected, even for very close bubbles ($z/d = 3$). The curves are quite flat and no increase in the rising velocity is present for smaller z/d values for all bubble diameters. As bubble diameter is grouped with a variation of ±0.05 mm in the equivalent diameter, this may explain in the data scatter. For example, bubbles grouped as $d \leqslant 0.25$ mm ranges from 0.12 to 0.23 mm, and as is known the rising velocity increases as the diameter increases. Typical pictures of bubbles are shown in Fig. 5 for frequencies of 40, 90 and 125 Hz from top-to-bottom.

The average rising velocity of a single bubble is calculated as follows. We cut out the first 1/3 of the path, and, in the remaining region, neglect bubbles with few acquisition steps or those with an unclear trajectory (negative velocity in a step, acquisition stopped when the bubble position is too low). The software checks for each bubble the linear best-fit gradient and accepts only those bubbles with a velocity gradient less than 6 s^{-1} and a velocity variation less than 20%. Eventually, if the gradient is lower, the graph $V = f(y)$, where y is the distance from the generation point, is shown for final manual check. Checking the plateau we can be sure that we only analyze the region where $V = V_T$. Discarded tests because of the non-reasonable gradient are those where the velocity is changed because the plateau is not reached, or there were disturbances in the fluid, or the bubble changes its trajectory, and the field taken in the movie does not allow the evaluation of

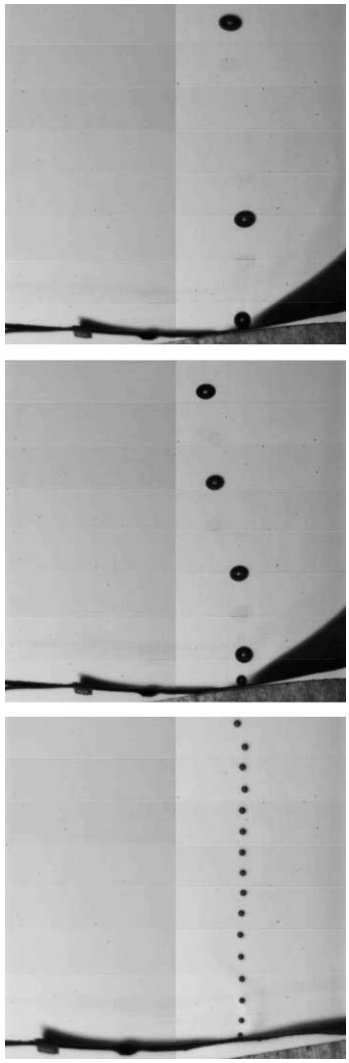

Fig. 5. Typical pictures of bubbles obtained at 40 Hz (top), 90 Hz (middle) and 125 Hz (bottom).

the terminal velocity. Fig. 6 shows typical plots of the bubble velocity trend as a function of the distance from the generation point together with the region neglected in the terminal velocity calculation (equal to 1/3 of the total bubble path) and the curves of the linear regression (best-fit) and the mean value.

An overall representation of all frequency controlled tests is given in Fig. 7, in which the bubble terminal rising velocity, V_T and the Weber number, We ($= \rho_l V_T^2 d/\sigma$) are plotted against either the equivalent bubble diameter, d, or the Eötvös number, Eo. For FC-72 data, we can see how V_T increases almost linearly with d, until this latter is smaller than about 0.4 mm, to which corresponds a value of Eo around 0.34 and We around 2.0. This value of the Eötvös number is in good agreement with the evaluation made using equations given by Tomiyama et al. (1998a), based on

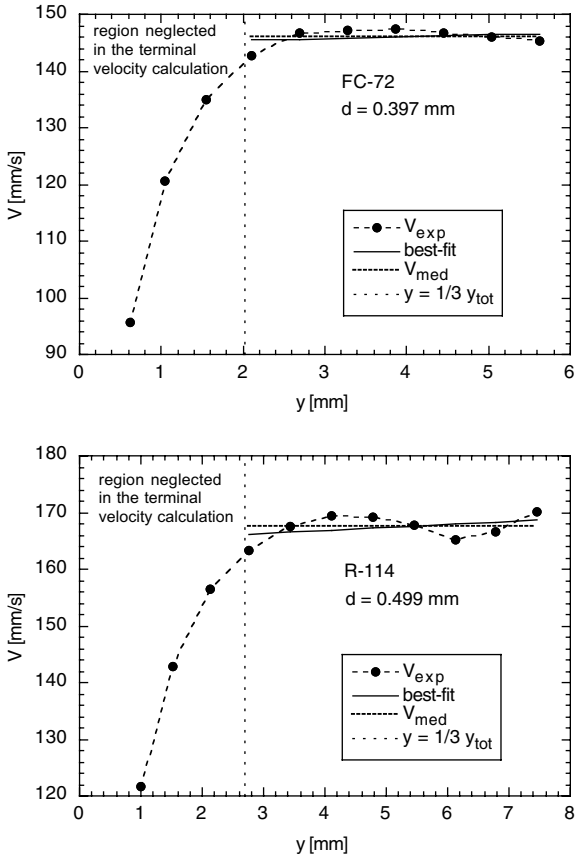

Fig. 6. Procedure of calculation of the (average) bubble terminal velocity.

Eötvös and Morton numbers, which yields a value of 0.32. This value of the Eötvös number or the equivalent bubble diameter (0.4 mm) represents the coordinates of the peak in the V_T–Eo (or V_T–d) curve.

Data scatter is not properly due to the experimental uncertainty but to the actual different behaviour of bubbles with the same equivalent diameter generated in different tests and to the different characteristics of the bubbles generated with the heating system, and this cannot be simply calculated.

Although the peak does not necessarily represents the transition between the viscosity and the surface tension dominant regime in the bubble motion, nonetheless the zone around the peak is a region where drastic changes in the bubble dynamics occur. As is known, the viscous force dominant regime (typically governing the motion of small spherical bubbles) is characterized by a drag coefficient, C_D, mainly depending on Reynolds number, Re. In the surface tension dominant regime (typically governing the motion of intermediate size bubbles), in turns, the drag coefficient mainly depends on the Eötvös number.

Therefore, for $Eo < 0.3$, where we have small bubbles almost spherical, we may say that bubble motion is mainly governed by the viscous force, where V_T increases with d and Eo, while for

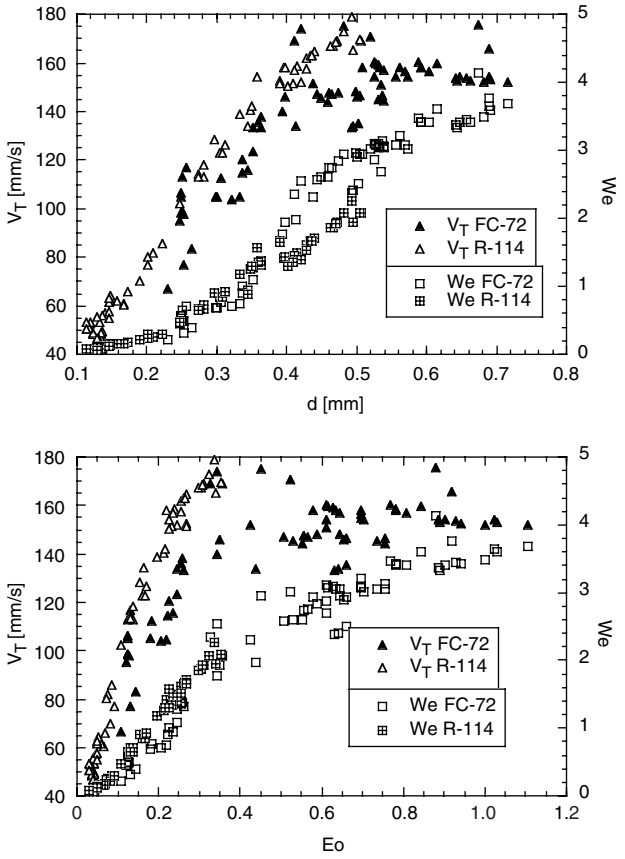

Fig. 7. Terminal rising velocity V_T and Weber number as a function of the mean equivalent diameter and the Eötvös number.

$Eo > 0.4$ surface tension force becomes more important. In this latter case, if shape oscillation does not take place, C_D is almost independent of bubble diameter (and Eo).

For $Eo > 0.3$, the scatter of V_T data (always for FC-72) is rather small. If we consider that the primal cause of large scatter of V_T in the surface tension force dominant regime may be the difference in initial shape deformation (Tomiyama et al., 2002), especially in contaminated liquid, though the process liquid is a pure fluid, we might conclude that bubble generation in present experiment is accompanied with rather low initial shape deformation. On the other hand, even in a pure system (where it is more difficult not to deform the bubble at the formation thus making less evident such effect) if we supply a strong deformation in the bubble at the formation it is possible to have a large evidence of the effect of the bubble initial deformation. This can be also confirmed from pictures shown in Fig. 5. Some pseudo-oscillation may be actually due to helical or zigzag trajectory of the bubbles, while the movie is taken in a 2-D situation. Such a motion, showing different parts of the bubbles, simulates shape oscillation.

Such considerations find full application to FC-72 data, which extend to both regions with $Eo < 0.3$ and $Eo > 0.4$. Most of the R-114 data instead, lie in the viscous force dominant regime

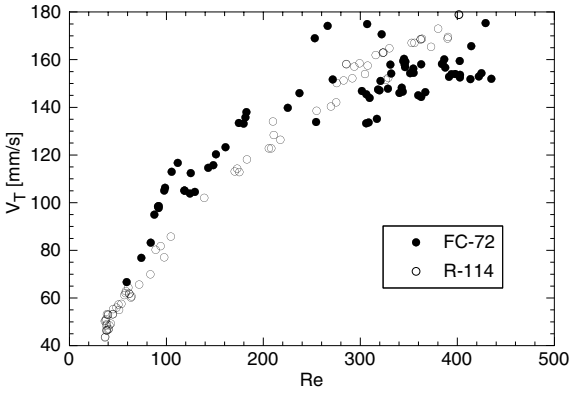

Fig. 8. Terminal rising velocity V_T as a function of the Reynolds number.

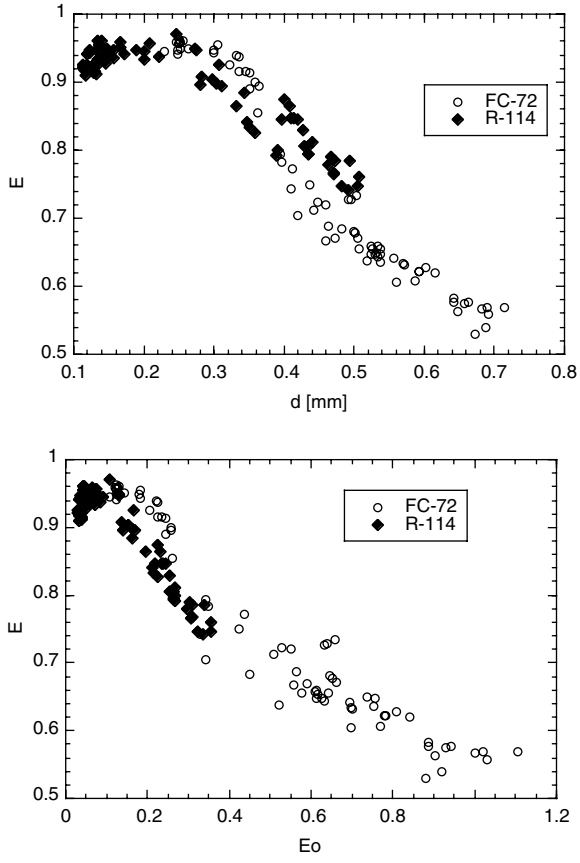

Fig. 9. Aspect ratio E as a function of the mean equivalent diameter and the Eötvös number.

and, although data exhibit some changes in the trend, the lack of data for $Eo > 0.35$ prevents us from extending the above discussion to this fluid.

The terminal velocity is also plotted versus the Reynolds number in Fig. 8. The velocity increases almost continuously with Reynolds number and R-114 exhibits a more regular trend. FC-data are more scattered especially at the highest values of the Reynolds number. However, the threshold above identified for $d = 0.4$ mm and $Eo = 0.32$, corresponds to $Re = 255$.

The aspect ratio, defined as the ratio between the minor (vertical) axis (h) and the major (horizontal) axis (b) of the bubble, $E = h/b$, is reported in Fig. 9, where E is plotted as a function of the bubble diameter, d, and Eötvös number, Eo, respectively. The aspect ratio is close to unity (almost spherical bubble) for $d < 0.3$ mm (for both FC-72 and R-114), then tends to decrease (bubble deformation) as d increases. It is interesting to notice that, for the values of d (about 0.45 mm) and Eo (about 0.32) for which we have the peak value in the V_T–d or V_T–Eo diagram for FC-72, we have a change in the slope of the E–d or E–Eo curve, respectively. The observation can hardly be extended to R-114 data, as they do not go beyond $Eo = 0.35$.

4. Data analysis

Data analysis has been accomplished using available correlations and models from the literature for the calculation of the bubble terminal rising velocity, V_T, and the aspect ratio, E.

4.1. Terminal rising velocity

A bubble moving freely in a liquid under the influence of gravity will rise at a constant velocity after the terminal condition is reached. From the balance of drag and buoyancy forces, the main important forces governing the motion of the bubble at the equilibrium, we have:

$$C_D \frac{1}{2}\rho_l V_T^2 \frac{\pi d^2}{4} = (\rho_l - \rho_g) g \frac{\pi d^3}{6} \tag{1}$$

Solving for V_T^2 yields:

$$V_T^2 = \frac{4(\rho_L - \rho_G) g d}{3 C_D \rho_L} \tag{2}$$

In order to calculate V_T, we have to evaluate C_D. For distorted bubbles under the condition of $Eo < 16$ (for the present data Eo is always less than 2.2 for FC-72 and less than 1.2 for R-114), Ishii and Chawla (1979) suggested the following simple correlation:

$$C_D = \frac{2}{3}\sqrt{Eo} \tag{3}$$

A more general equation was proposed by Ishii and Chawla (1979) as follows:

$$C_D = \max\left\{ \frac{24}{Re}(1 + 0.1 Re^{0.75}), \min\left[\frac{2}{3}\sqrt{Eo}, \frac{8}{3} \right] \right\} \tag{4}$$

Wallis (1974) proposed:

$$C_D = \max\left\{ \min\left[\max\left(\frac{16}{Re}, \frac{13.6}{Re^{0.8}} \right), \frac{48}{Re} \right], \min\left[\frac{Eo}{3}, 0.47 Eo^{0.25} We^{0.5}, \frac{8}{3} \right] \right\} \tag{5}$$

Tomiyama et al. (1998a) considering that the value of C_D for distorted bubbles becomes larger than that for spherical bubbles, recommend to use the larger value of the two drag coefficients for the two situations among those obtained using available correlations. The following expressions for C_D to be used with Eq. (2) are therefore recommended:

(a) For a pure system:

$$C_D = \max\left\{ \min\left[\frac{16}{Re}(1+0.15Re^{0.687}), \frac{48}{Re}\right], \frac{8}{3}\frac{Eo}{Eo+4}\right\} \tag{6}$$

(b) For a slightly contaminated system:

$$C_D = \max\left\{ \min\left[\frac{24}{Re}(1+0.15Re^{0.687}), \frac{72}{Re}\right], \frac{8}{3}\frac{Eo}{Eo+4}\right\} \tag{7}$$

(c) For a fully contaminated system:

$$C_D = \max\left[\frac{24}{Re}(1+0.15Re^{0.687}), \frac{8}{3}\frac{Eo}{Eo+4}\right] \tag{8}$$

Some other researchers have proposed models for the direct prediction of the terminal rising velocity, V_T. Chronologically, Mendelson (1967) related the rise velocity of bubbles to the hydrodynamic theory of waves, providing the following equation for the direct calculation of the terminal rising velocity, V_T, which is valid for intermediate-large bubbles:

$$V_T = \sqrt{\frac{2\sigma}{d\rho_l} + \frac{\Delta\rho}{\rho_l}\frac{gd}{2}} \tag{9}$$

$\Delta\rho$ is the difference between liquid and gas density.

Fan and Tsuchiya (1990) developed a general correlation for the prediction of bubble terminal rising velocity which is applicable to both pure and contaminated systems, and provides a continued correlation for the viscous force and surface tension dominant regimes:

$$V_T = (V_{T1}^{-n} + V_{T2}^{-n})^{-1/n} \tag{10}$$

where V_{T1} and V_{T2} are the expressions for terminal speed in the viscous regime and in the distorted/cap bubble (surface tension dominant) regime. They are given by:

$$V_{T1} = \frac{\rho_l g d^2}{K_b \mu_l}, \quad V_{T2} = \sqrt{\frac{2c\sigma}{d\rho_l} + \frac{gd}{2}} \tag{11}$$

The three parameters n, c and K_b reflect three specific factors governing the rate of bubble rise. They relate to the contamination level of the liquid phase, to the varying dynamic effects of the surface tension, and to the viscous nature of the surrounding medium

$$K_b = \max(12, K_{bo} Mo^{-0.038}), \quad Mo = \frac{\Delta\rho g \mu_l^4}{\sigma^3 \rho_l^2} \tag{12}$$

where K_{bo} is equal to 14.7 for aqueous solutions and 10.2 for organic solvents/mixtures, and Mo is the Morton number. Concerning the other two parameters, n is equal 0.8 for contaminated liquids

(a smaller value is suggested for hot tap water) and 1.6 for purified liquids, while c is equal to 1.2 for mono-component liquids and 1.4 for multi-component liquids. Eq. (10) satisfies the condition that V_{T1} dominates when d is small, and V_{T2} dominates when d is large. If $c = 1$, then V_{T2} is practically coincident with the Mendelson (1967) correlation.

Recently, a new model for the prediction of the terminal velocity on bubbles in the surface tension force dominant regime was proposed by Tomiyama et al. (2002). The model is based on the assumption of a distorted oblate spheroidal shape and the extension of the potential flow solution for a flow around a sphere (Davies and Taylor, 1950) by taking the surface tension effect into account:

$$V_T = \frac{f(m,E)}{\sqrt{(1-E^2)(1-m^2)}} \frac{\sin^{-1}\sqrt{(1-E^2)} - E\sqrt{(1-E^2)}}{(1-E^2)} \times \sqrt{\frac{4\sigma}{\rho_l d}\frac{E^{4/3}}{\gamma^{1/3}}\left[\frac{1}{f(m,E)} + \frac{1}{f(m,E)^3} - 2\right] + \frac{\Delta\rho g d}{\rho_l}\gamma^{1/3}E^{2/3}(1-m)} \tag{13}$$

$$f(m,E) = \sqrt{m^2 + E^2(1-m^2)}, \quad m = \cos\phi$$

where ϕ is the angle from the vertical, γ the distortion factor, assuming in general a non fore-aft symmetric ellipsoidal bubble (Tomiyama et al., 2002). According to Clift et al. (1978) when the bubble Reynolds number, Re, is high, the potential flow theory is valid not only in the vicinity of the bubble nose but also up to a certain large angle ϕ from the vertical line, e.g. $\phi \sim 160°$. Hence there is a possibility to obtain a good evaluation of the terminal velocity V_T by specifying an appropriate angle ϕ for each particular problem. Tomiyama et al. (2002) calculated the above equation for $\phi \to 0$; i.e., assuming that the potential flow is valid only in the vicinity of the bubble nose. Under the assumption of a symmetric bubble, the above condition yields:

$$V_T = \frac{\sin^{-1}\sqrt{(1-E^2)} - E\sqrt{(1-E^2)}}{1-E^2}\sqrt{\frac{8\sigma}{\rho_l d}E^{4/3} + \frac{\Delta\rho g d}{2\rho_l}\frac{E^{2/3}}{1-E^2}} \tag{14}$$

Predictions obtained using the above-described correlations and models are compared with experimental data in Figs. 10–13. Fig. 10 shows the ratio between the calculated and measured bubble terminal rising velocities versus the equivalent bubble diameter, for FC-72 and R-114 data.

Tomiyama et al. (2002) model and Fan and Tsuchiya (1990) correlation show the best agreement with experimental data. As far as the Tomiyama et al. model is concerned, predictions are obtained assuming $\gamma = 1$ (symmetric ellipsoidal bubble), and fixing the angle ϕ equal to 145°. This value has been obtained on a different data set always using FC-72 and R-114 (Celata et al., 2001b) and used for present data. Predictions using the Fan and Tsuchiya correlation are obtained by setting K_{bo} equal to 10.2 (organic solvents/mixtures), n equal 1.6 (purified liquids), and c equal to 1.4 (multi-components liquids). The above parameters n, c and K_{bo} are directly taken from the original formulation, and are not adjusted on present data. Successful employ of Fan and Tsuchiya correlation for refrigerants with the same parameters values have been claimed by Vassallo et al. (1995).

Considering the FC-72 data, the Tomiyama et al. model exhibits a slight overestimation of data (less than 10%) while the Fan and Tsuchiya correlation slightly underpredicts data (less than

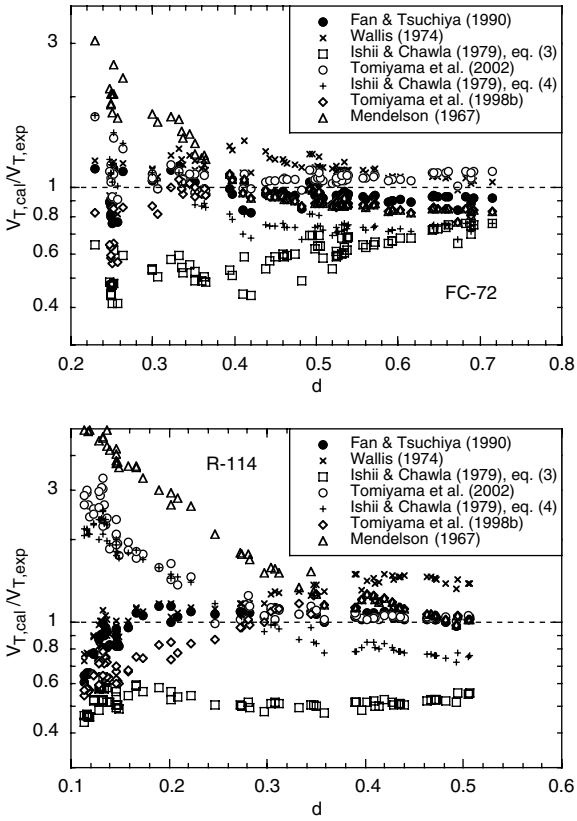

Fig. 10. Predictions of present data using available models as a function of the bubble equivalent diameter, d, for FC-72 (top) and R-114 (bottom).

10%). Both predictive tools tend to increase the error as the bubble diameter decreases to very small values ($d < 0.2$ mm). This latter behaviour is more apparent for R-114 data, where we have more bubbles less than 0.2 mm in diameter. On the contrary, the prediction of R-114 data is excellent for both predictive tools for $d > 0.2$ mm.

The other correlations tested here provides less favourable predictions of both sets of data; Wallis (1974) correlation predicts reasonably well data for $d < 0.3$ mm, while it overpredicts FC-72 (slightly) and R-114 data for $d > 0.3$. Mendelson (1967) correlation exhibits a behaviour very similar to the Fan and Tsuchiya correlation (as expected) for $d > 0.4$–0.5 mm, while largely overpredicts data for smaller diameters. Therefore, further plots of data predictions will show only predictions obtained with Fan and Tsuchiya (1990) correlation and Tomiyama et al. (2002) model and Wallis (1974) correlation.

The ratio between the calculated and measured bubble terminal rising velocities versus the Eötvös number, *Eo*, for FC-72 and R-114 data, is shown in Fig. 11. The trend is similar to that as a function of the bubble diameter, but the behaviour of each model/correlation is more evident due to the reduced number of predictive tools.

Predictions are also plotted in a similar way in Fig. 12 as a function of the Weber number, *We*. The Fan and Tsuchiya correlation and Tomiyama et al. model show a good prediction of both

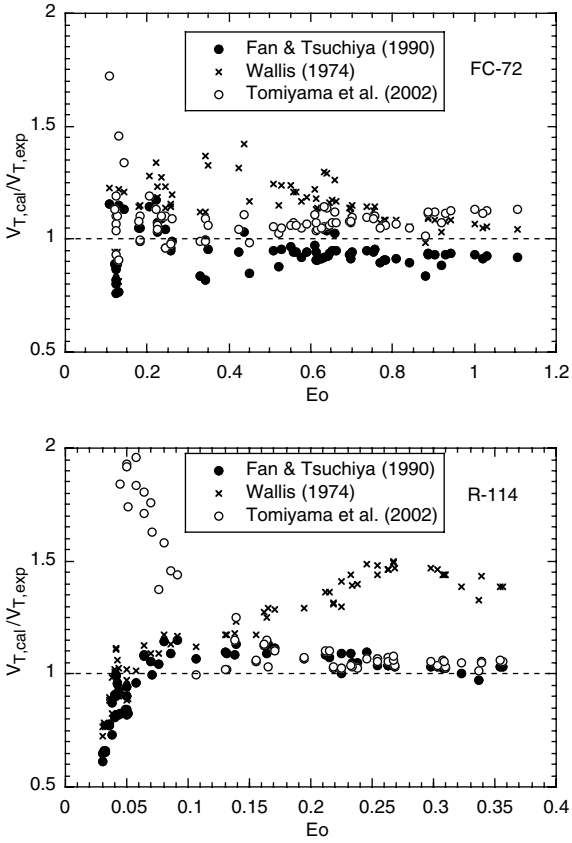

Fig. 11. Predictions of present data using available models as a function of Eötvös number, *Eo*, for FC-72 (top) and R-114 (bottom).

data sets as long as *We* is greater than 0.5. The Wallis correlation would seem to have a systematic error depending on *We*. It is interesting to remark here that for FC-72 data ranging from $We = 2$ to $We = 4$, the Wallis correlation provides $C_D = Eo/3$. Therefore, considering Eqs. (2) and (5) we have that $V_{T,cal}/V_{T,exp} = 2/We^{0.5}$, i.e., exactly the trend observed in the figure. The same happens with R-114 data for $We > 1.8$. Finally, same predictions are shown in Fig. 13 as a function of the aspect ratio, *E*. Fan and Tsuchiya correlation and Tomiyama et al. model start deviating from a good prediction of data when the aspect ratio is greater than 0.9. This is typical to tiny bubbles which tends to be almost spherical. This had to be expected from the use of the Tomiyama et al. model, as this has been developed for distorted bubbles in the surface tension dominant regime. On the contrary, the Fan and Tsuchiya correlation should hold for small spherical bubbles, and its large underprediction is unexpected.

4.2. Aspect ratio

Several attempts have been made in the literature to correlate the aspect ratio, *E*, as a function of a dimensionless parameter which could group the experimental data. Some authors have tried

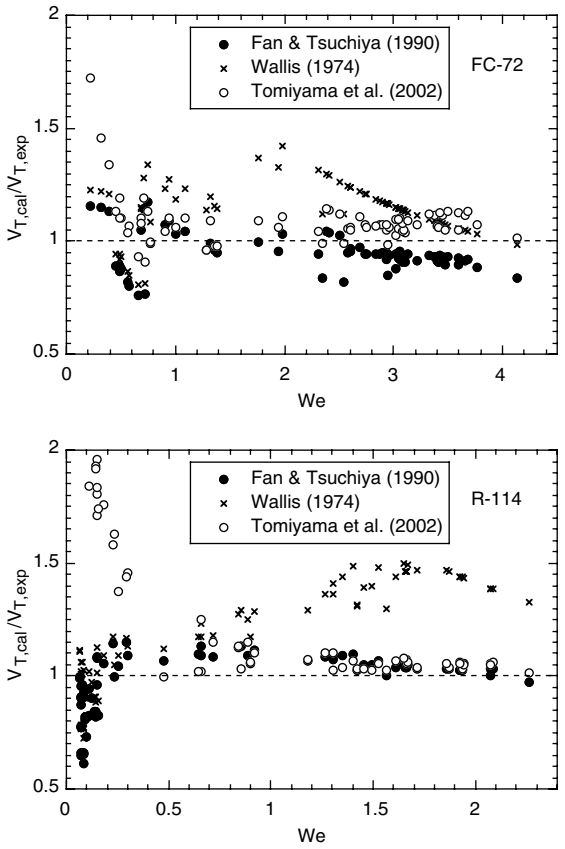

Fig. 12. Predictions of present data using available models as a function of Weber number, *We*, for FC-72 (top) and R-114 (bottom).

to accomplish this task using the Eötvös number, *Eo* (Wellek et al., 1966, Okawa et al., 2003), others have tried to use the Weber number, *We* (Moore, 1959, Wellek et al., 1966, and Taylor and Acrivos, 1964), while some other have used the Tadaki number, *Ta*, defined as a function of the Reynolds and the Morton number, $Ta = ReMo^{0.23}$. Other dimensionless parameters, such as the Reynolds and Morton numbers are not successful in correlating present data.

Tomiyama et al. (2001) measuring the rising velocity of air bubbles in stagnant water observed that the aspect ratio, which depends on the magnitude of initial shape oscillation, has strong correlation with the Weber number.

Correlations based on the Eötvös number, *Eo*, have been found to be largely dependent on the method of bubble formation, i.e., the condition at the detachment (Tomiyama et al., 2001, Okawa et al., 2003), and are therefore bounded to give good predictions of *E* for very small bubbles.

According to Fan and Tsuchiya (1990), Wellek et al. (1966) correlation

$$E = \frac{1}{1 + 0.163 Eo^{0.757}} \tag{15}$$

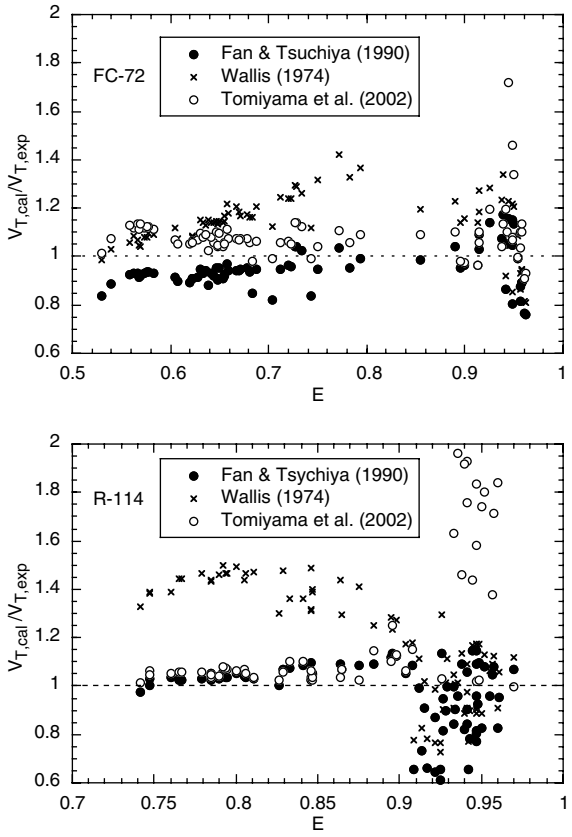

Fig. 13. Predictions of present data using available models as a function of the aspect ratio, E, for FC-72 (top) and R-114 (bottom).

which was originally developed for nonoscillating drops in contaminated liquids, appears to be extendible even to oscillating bubbles in low-viscosity liquids.

Recently, Okawa et al. (2003) modified the Wellek et al. correlation, providing a lower boundary of their data:

$$E = \frac{1}{1 + 1.97 Eo^{1.3}} \tag{16}$$

The comparison between the above correlations and measured data is shown in Fig. 14, where E is plotted against Eo. As already observed by Tomiyama et al. (2001) and Okawa et al. (2003), the Eötvös number is not the most appropriate parameter to group bubble shape data, although present data are not very much scattered. Wellek et al. (1966) correlation provides an upper boundary of FC-72 and R-114 data and correlates these data fairly well, as expected, until bubbles are almost spherical ($E \geqslant 0.95$), corresponding to $Eo \approx 0.25$. Also for present data Okawa et al. (2003) correlation provides a lower boundary.

Predictive tools based on the Weber number, *We*, have been found to be more adequate to collapse aspect ratio data, evidencing that the bubble shape is largely affected by inertia and

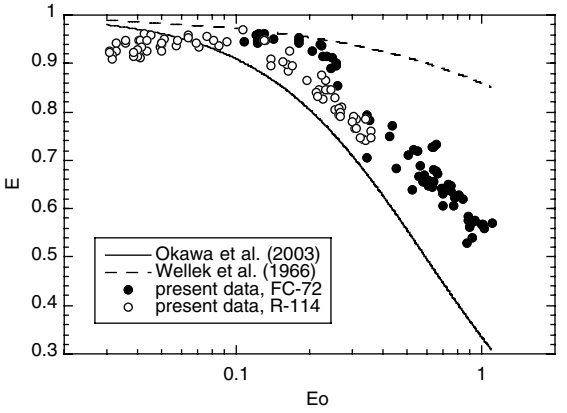

Fig. 14. Prediction of the aspect ratio using the Eötvös number based correlations, Wellek et al. (1966) and Okawa et al. (2003).

surface tension. Moore (1959), for bubbles which do not deviate largely from a spherical shape, and assuming that the flow around the entire bubble surface is essentially inviscid (he noted that for $Re > 200$ the shape is independent of viscous effect), derived the following model:

$$We = \frac{4(R_E^3 + R_E - 2)[R_E^2 \sec^{-1} R_E - (R_E^2 - 1)^{1/2}]^2}{R_E^{4/3}(R_E^2 - 1)^3} \tag{17}$$

where R_E defined as the inverse of the aspect ratio E.

Taylor and Acrivos (1964) proposed a theory for creeping flow (low Reynolds number) which can be developed as a series; considering only the first term of the series we have:

$$E = \frac{1}{1 + \frac{5}{32} We} \tag{18}$$

Wellek et al. (1966), for nonoscillating liquid drops in fairly contaminated liquids proposed the following correlation based on *We*:

$$E = \frac{1}{1 + 0.091 We^{0.95}} \tag{19}$$

Fig. 15 shows the plot of E as a function of *We*, along with predictions provided by Moore (1959) correlation, Taylor and Acrivos (1964) equation, and Wellek et al. (1966) correlation. The Weber number, compared with the Eötvös number, seems to be a suitable parameter to correlate bubble shape. Both FC-72 and R-114 data lie on the same curve in the *E–We* plot. Globally, the best prediction of the aspect ratio as a function of *We* is given by Taylor and Acrivos (1964) theory, although it has been developed in a completely different range of validity. It slightly underestimates the FC-72 data for $We \approx 1$, and overpredicts data for $We > 3$ and for $We < 0.2$. Moore (1959) correlation is coincident with the Taylor and Acrivos predictions until $We = 0.7$, then underestimates data. Finally, Wellek et al. (1966) correlation generally overestimates experimental data.

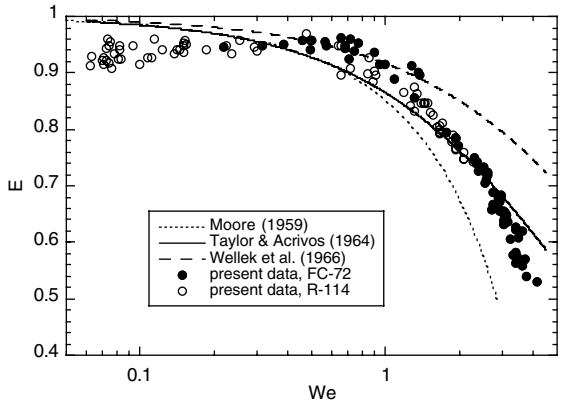

Fig. 15. Prediction of the aspect ratio using the Weber number based correlations, Moore (1959), Taylor and Acrivos (1964), and Wellek et al. modified by Fan and Tsuchiya (1990).

The Tadaki number, *Ta*, has been used by some researchers to predict the bubble shape. Tadaki and Maeda (1961) found experimentally that, for all liquids they tested ($Mo < 2.5 \times 10^{-4}$), except surfactant solutions, the relationship between d/b, where d is the equivalent diameter of the bubble and b is the major (horizontal) axis of the bubble, and the Reynolds number was a unique function of the Morton number, *Mo*, and d/b could be correlated with a single parameter, the Tadaki number (Clift et al., 1978). It is noted that d/b is equal to $E^{1/3}$ for ellipsoidal bubbles. They proposed the following relationship for the calculation of the aspect ratio as a function of the Tadaki number. Fan and Tsuchiya (1990) demonstrated that the Tadaki number is either a function of the Weber and the Froude number, or a function of the Eötvös and the Froude number, being the Froude number given by $Fr = V_T^2/gd$. This is equivalent to say that the bubble shape (for low-*Mo* liquids) can be determined from the balance among surface tension, inertial and gravity forces; viscous forces are negligible. The Tadaki and Maeda correlation is expressed as:

$$E^{1/3} = \begin{cases} 1 & Ta < 2 \\ 1.14\,Ta^{-0.176} & 2 < Ta < 6 \\ 1.36\,Ta^{-0.28} & 6 < Ta < 16.5 \\ 0.62 & 16.5 < Ta \end{cases} \tag{20}$$

Later, Vakhrushev and Efremov (1970) modified Tadaki and Maeda (1961) correlation as follows:

$$E = \begin{cases} 1 & Ta < 0.3 \\ \{0.77 + 0.24\tanh[1.9(0.40 - \log_{10} Ta)]\}^2 & 0.3 < Ta < 20 \\ 0.30 & 20 < Ta \end{cases} \tag{21}$$

The aspect ratio is plotted versus the Tadaki number, along with Tadaki and Maeda (1961) and Vakhrushev and Efremov (1970) correlations in Fig. 16. The Tadaki number might be an appropriate parameter in correlating the aspect ratio, as data lie on the same curve in the *E*–*Ta* plot, though Tadaki and Maeda (1961) correlation is definitely inadequate to predict the present

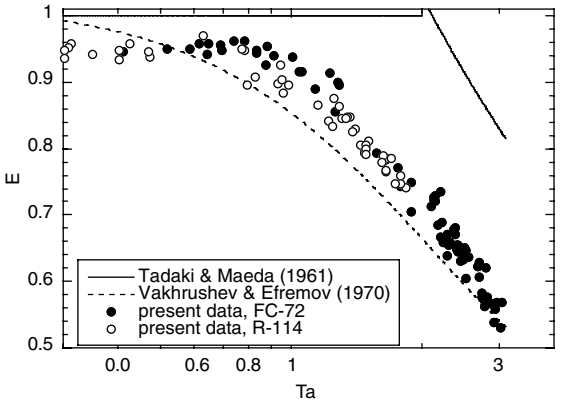

Fig. 16. Prediction of the aspect ratio using the Tadaki number based correlations, Tadaki and Maeda (1961), and Vakhrushev and Efremov (1970).

data. Better predictions are provided by the Vakhrushev and Efremov (1970) correlation, though it would seem to be not as good as Taylor and Acrivos (1964) theory (in the *E–We* plot).

The best dimensionless parameter to correlate bubble shape in the present experiment (refrigerant vapour-liquid data) would therefore be the Weber number, and, specifically, the equation developed from Taylor and Acrivos (1964) theory shows the best agreement with the present data, confirming that the bubble shape is controlled by inertia and surface tension.

5. Conclusions

An experiment of bubble rising velocity has been performed using FC-72 and R-114 as test fluids. Bubbles are generated directly in the saturated liquid using a heater placed at the bottom of the test chamber where the liquid is first heated up to saturation conditions, representing a one-component system which has not been extensively studied so far. Single bubble and bubble train with controlled frequency tests have been conducted in the range of bubble diameter from 0.1 to 0.7 mm. The research is focused on the analysis of the wake effect on the bubble terminal rising velocity in this range of bubble diameter. As it could be somewhat argued from Tsuge and Hibino (1972) data, referring to bubble diameters from about 9 to 5 mm, and from Marks (1973) experiments, the wake effect can be considered negligible for such small bubbles. Experiments have clearly shown an evidence of the absence of the wake effect.

Experimental data shows that the surface tension force plays a dominant role in the terminal rising velocity for bubbles larger than about 0.4–0.5 mm in diameter (depending somewhat on the fluid), corresponding to an Eötvös number equal to 0.32, while the viscous force play a decisive role for smaller bubbles.

The terminal velocity can be predicted with an acceptable accuracy with Fan and Tsuchiya (1990) correlation and Tomiyama et al. (2002) model. Both fail in predicting data with a bubble diameter less than 0.2 (corresponding to $Eo = 0.12$ and $We = 0.9$), and an aspect ratio larger than 0.9. It has to be said here that Tomiyama et al. model is expected to exhibit such a behaviour as it

has been developed mainly for distorted spheroidal bubbles in the surface tension dominant regime. Other correlations available are inadequate to correlate the present data. It is necessary to say here that all of them are developed for two-component systems, i.e., gas–liquid.

The bubble shape (aspect ratio) can be well correlated in terms of Weber number, as outlined by Tomiyama et al. (2001), as well as using the Tadaki number. Among several available predictive tools, Taylor and Acrivos (1964) theory gives the best prediction. Vakhrushev and Efremov (1970) correlation also gives reasonable predictions.

Acknowledgements

Authors are very grateful to Prof. Paolo Di Marco for the continuous and fruitful discussion in the preparation of this paper.

References

Bhaga, D., Weber, M.E., 1981. Bubbles in viscous liquids: shape, wakes and velocities. J. Fluid Mech. 105, 61–85.

Celata, G.P., Cumo, M., D'Annibale, F., Tomiyama, A., 2001a. Bubble rising velocity in saturated liquid up to the critical pressure. In: Proceedings of 5th World Conference on Experimental Heat Transfer, Fluid Mechanics and Thermodynamics, vol. II, Thessaloniki, pp. 1319–1328.

Celata, G.P., Cumo, M., D'Annibale, F., Tomiyama, A., 2001b. Terminal bubble rising velocity in one-component systems. In: European Two-Phase Flow Group Meeting, Paper F3, Aveiro, 18–20 June 2001.

Clift, R., Grace, J.R., Weber, M.E., 1978. Bubbles, Drops and Particles. Academic Press, New York.

Davies, R.M., Taylor, G., 1950. The mechanics of large bubbles rising through extended liquids and through liquids in tubes. Proc. Roy. Soc. Lond., Ser. A 200, 375–390.

Di Marco, P., Grassi, W., Memoli, G., 2003. Experimental study on rising velocity of nitrogen bubbles in FC-72. Int. J. Therm. Sci. 42, 435–446.

Fan, L.S., Tsuchiya, K., 1990. Bubble Wake Dynamics in Liquids and Liquid–Solid Suspensions. Butterworth-Heinemann, Oxford.

Fan, L.S., Yang, G.Q., Lee, D.J., Tsuchiya, K., Luo, X., 1999. Some aspects of high-pressure phenomena of bubbles in liquids and liquid–solid suspensions. Chem. Engng. Sci. 54, 4681–4709.

Grace, J.R., Wairegi, T., Nguyen, T.H., 1976. Shapes and velocities of single drops and bubbles moving freely through immiscible liquids. Trans. IChemE 54, 167.

Ishii, M., Chawla, T.C., 1979. Local drag laws in dispersed two-phase flow, ANL-79-105.

Katz, J., Menevau, C., 1996. Wake-induced relative motion of bubbles rising in line. Int. J. Multiphase Flow 22, 239–258.

Kupferberg, A., Jameson, G.J., 1969. Bubble formation at submerged orifice above a gas chamber of finite volume. Trans. IChemE 47, 241–250.

Marks, C.H., 1973. Measurements of the terminal velocity of bubbles rising in a chain. J. Fluid Engng. 95, 17–22.

Mendelson, H.D., 1967. The prediction of bubble terminal velocities from wave theory. AIChE J. 13, 2150.

Moore, D.W., 1959. The rise of a gas bubble in a viscous liquid. J. Fluid Mech. 6, 113–130.

Okawa, T., Tanaka, T., Kataoka, I., Mori, M., 2003. Temperature effect on single bubble rise characteristics in stagnant distilled water. Int. J. Heat Mass Transfer 46, 903–913.

Park, Y., Lamont Tyler, A., de Nevers, N., 1977. The chamber orifice interaction in the formation of bubbles. Chem. Engng. Sci. 32, 907–916.

Peebles, F., Garber, H., 1953. Studies on the motion of gas bubbles in liquid. Chem. Engng. Progr. 49, 88–97.

Ruzicka, M.C., 2000. On bubbles rising in line. Int. J. Multiphase Flow 26, 1141–1181.

Satynarayan, A., Kumar, R., Kuloor, N.R., 1969. Studies in bubble formation—II. Bubble formation under constant pressure conditions. Chem. Engng. Sci. 24, 749–761.

Tadaki, T., Maeda, M., 1961. On the shape and velocity of single air bubbles rising in various liquids. Kagaku Kogaku 25, 254–264 (also cited by Fan and Tsuchiya, 1990).

Taylor, T.D., Acrivos, A., 1964. On the deformation and drag of a falling viscous drop at low Reynolds number. J. Fluid Mech. 18, 466–476.

Tomiyama, A., 1998. Struggle with computational bubble dynamics. In: Proceedings of 3rd International Conference on Multiphase Flows (CD-ROM), Lyon, 8–12 June.

Tomiyama, A., Celata, G.P., Hosokawa, S., Yoshida, S., 2002. Terminal velocity of single bubbles in surface tension force dominant regime. Int. J. Multiphase Flow 28, 1497–1519.

Tomiyama, A., Kataoka, I., Zun, I., Sakaguchi, T., 1998a. Drag coefficients of single bubbles under normal and microgravity conditions. JSME Int. J., Ser. B 41, 472–479.

Tomiyama, A., Miyoshi, K., Tamai, H., Zun, I., Sakaguchi, T., 1998b. A bubble tracking method for the predictions of spatial-evolution of bubble flow in a vertical pipe. In: Proceedings of 3rd International Conference on Multiphase Flows (CD-ROM), Lyon, 8–12 June.

Tomiyama, A., Yoshida, S., Hosokawa, S., 2001. Surface tension force dominant regime of single bubbles rising through stagnant liquid, UK-Japan Seminar on Multiphase Flow.

Tsuge, H., 1986. Hydrodynamics of Bubble Formation from Submerged Orifices. Encyclopaedia Fluid Mech., 191–232 (Chapter 9).

Tsuge, H., Hibino, S.I., 1972. The motion of gas bubbles generating from a single orifice submerged in a liquid. Keio Engng. Rep. 25.

Vakhrushev, I.A., Efremov, G.I., 1970. Chem. Techn. Fuel Oils (USSR) 5/6, 376–379 (cited by Clift et al., 1978).

Vassallo, P.F., Symolon, P.D., Moore, W.E., Trabold, T.A., 1995. Freon bubble rising measurements in a vertical rectangular duct. J. Fluids Engng. 117, 729–732.

Wallis, G.B., 1969. One-dimensional two-phase flow. Bubbly Flow, 243–281 (Chapter 9).

Wallis, G.B., 1974. The terminal speed of single drops or bubbles in an infinite medium. Int. J. Multiphase Flow 1, 491–511.

Wellek, R.M., Agrawal, A.K., Skelland, A.H.P., 1966. Shape of liquid drops moving in liquid media. AIChE J. 12, 854–862.